CHEMISTRY
A European Journal

A Journal of
ChemPubSoc Europe

## Accepted Article

**Title:** The Gold(I)-Mediated Domino Reaction to Fused Diphenyl Phosphoniumfluorenes: Mechanistic Consequences for Gold-Catalyzed Hydroarylations and the Application in Solar Cells

**Authors:** Sebastian Arndt, Jan Borstelmann, Rebeka Eshagh Saatlo, Patrick W. Antoni, Frank Rominger, Matthias Rudolph, Qingzhi An, Yana Vaynzof, and A. Stephen K. Hashmi

**To be cited as:** *Chem. Eur. J.* 10.1002/chem.201800460

**Link to VoR:** http://dx.doi.org/10.1002/chem.201800460

Supported by ACES

WILEY-VCH

# The Gold(I)-Mediated Domino Reaction to Fused Diphenyl Phosphoniumfluorenes: Mechanistic Consequences for Gold-Catalyzed Hydroarylations and the Application in Solar Cells

Sebastian Arndt,[a] Jan Borstelmann,[a] Rebeka Eshagh Saatlo,[a] Patrick W. Antoni,[a] Frank Rominger,[a] Matthias Rudolph,[a] Qingzhi An,[b,c] Yana Vaynzof,*[b,c] and A. Stephen K. Hashmi*[a,d]

**Abstract:** A domino sequence, involving a phosphinoauration and a gold-catalyzed *6-endo-dig* cyclization step, was developed. Starting from modular- and simple-to-prepare phosphadiynes, π-extended phosphoniumfluorenes were synthesized. The mechanistic proposal is supported by kinetic measurements and by the trapping of key-intermediates. These led to important conclusions for the gold-catalyzed hydroarylation mechanism. Cyclic voltammetry (CV) and UV-Vis measurements indicated interesting properties for material science. The phosphoniumfluorene structure was tested as a hole-blocking layer in perovskite solar cells of inverted architecture. Devices with the phosphoniumfluorene exhibit an efficiency of 14.2% which is much higher than that of devices without (10.7%).

## Introduction

Domino reactions allow the generation of structural complexity in a simple procedure.[1] Without the need for isolation of the intermediates, domino reactions enhance the efficiency and sustainability with respect to costs, time and waste production.[2] Among many examples of domino reactions in homogeneous gold-catalysis,[3,4] a phosphonylation-*6-endo-dig*-cyclization cascade has not yet been reported. This is due to the strong coordination ability of phosphanes to gold(I), inhibiting the catalyst effectively. Recently, we reported phosphinoauration[5] and protophosphonylation[6] reactions as tool for the synthesis of phosphindolium structures. By expanding the phosphane-tolane scaffolds with an additional alkyne moiety, we envisioned a possible cycloisomerization towards fused diphenyl phosphoniumfluorenes (Scheme 1). Phosphorus-containing fluorenes have recently become interesting molecules for organic materials as they act as stable electron acceptors at relatively low reduction potentials.[7] However, compared to oxo or thioxo phosphafluorenes,[8] the phosphoniumfluorene structure is largely unexplored to date. Only 2% of the literature covering phosphafluorenes comprises phosphoniumfluorenes, which might be attributed to the few preparative methods provided. A generally accepted synthesis of phosphonium salts is the addition of a forth substituent to a trivalent phosphane by nucleophilic substitution. But while the installation of a methyl[9] or benzyl[10] substituent is relatively simple, the coupling of an aryl substituent is challenging. It requires the catalytic employment of palladium[11] or nickel,[12] or stoichiometric reactions with *in situ*-generated arynes[13] or aryl radicals.[14] Only the aryne method has been used for the modification of a phospha- to a phosphoniumfluorene by Chatani and coworkers.[15,16] Using this method, a low isolated yield (27%) was achieved for the simplest diphenyl phosphoniumfluorene, which demonstrates the difficulty of phosphafluorene modifications. A direct synthesis was described by Widhalm *et al.*[17] They obtained a phosphoniumfluorene in a high yield through a twofold halogen-metal exchange of a 2,2'-dibromo binaphthyl and a subsequent addition of chlorodiphenylphosphane. Although this method could be a key-approach to phosphoniumfluorenes, only one example was mentioned and more complex biaryl-scaffolds might be expensive to synthesize. The most advanced strategy was reported by Wang *et al.* just recently. They developed a powerful copper-mediated method for the synthesis of versatile phospholium structures. However, the major drawback is the consumption of two equivalents of the copper salt which finally ends up as a byproduct.[18] Herein, we report a mild and simple access to π-extended diphenyl phosphoniumfluorenes.

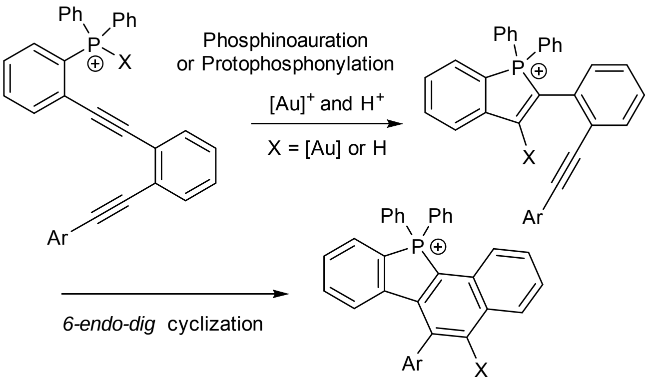

**Scheme 1.** Domino sequence. Counter anions are omitted.

## Results and Discussion

Our initial experiments addressed the assignment of the intermittent phosphindolium species. Therefore, stoichiometric amounts of gold(I) were used and the reactions were conducted without the addition of acids. [Phosphadiyne-Au(NHC)][X] **1a-Au** was generated *in situ* by dissolving the enediyne **1a** and 1 eq. of

---

[a] Organisch-Chemisches Institut, Ruprecht-Karls-Universität Heidelberg, Im Neuenheimer Feld 270, 69120 Heidelberg (Germany).
[b] Kirchhoff-Institute for Physics, Ruprecht-Karls-Universität Heidelberg, Im Neuenheimer Feld 227, 69120 Heidelberg (Germany).
[c] Centre for Advanced Materials, Ruprecht-Karls-Universität Heidelberg, Im Neuenheimer Feld 225, 69120 Heidelberg (Germany).
[d] Chemistry Department, Faculty of Science, King Abdulaziz University (KAU), Jeddah 21589, Saudi Arabia.
* E-mail: hashmi@hashmi.de, vaynzof@uni-heidelberg.de

Supporting information for this article is given via a link at the end of the document.

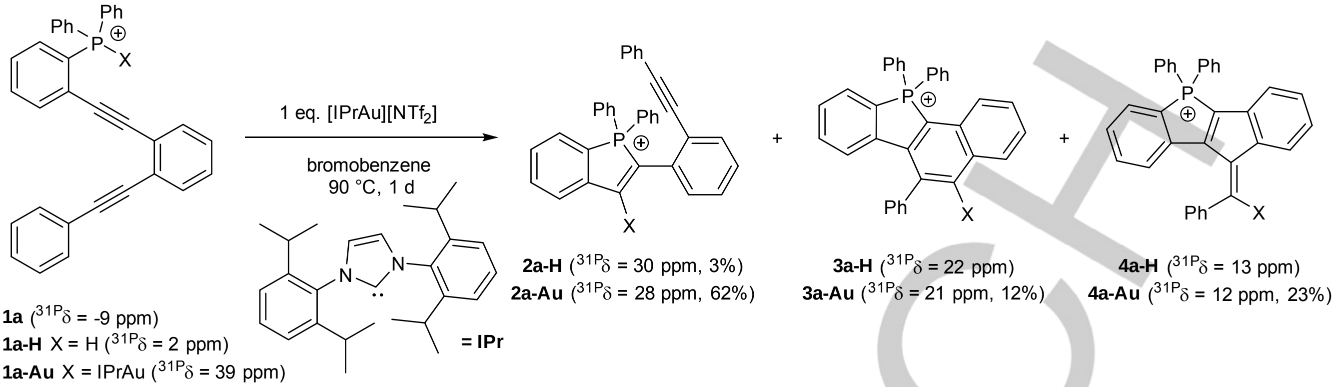

**Scheme 2.** Initial reaction and structural assignment. Counter anions ($NTf_2^-$) are omitted for clarity.

[IPrAu][NTf$_2$] in bromobenzene. The P-Au bond was clearly established as confirmed by $^{31}$P NMR spectroscopy ($\delta$ = 38.5 ppm). Upon heating to 90 °C, the $^{31}$P NMR monitoring revealed the generation of mainly four species with chemical shifts at $\delta$ = 30 ppm, 28 ppm, 21 ppm, and 12 ppm (ratio = 3:62:12:23; Scheme 2). The signals at $\delta$ = 30 ppm and $\delta$ = 28 ppm were assigned to the phosphindolium salts **2a-H** and **2a-Au**. The signal at $\delta$ = 21 ppm was assigned to the desired **3a-Au**. Later, a crystal structure of another derivative revealed that the species resonating at $\delta$ = 12 ppm (**4a-Au**) can be assigned to the *5-exo-dig* cyclization product. Further experiments addressing the protodeauration of the intermediate species gave signals at $\delta$ = 22 ppm and $\delta$ = 13 ppm, which were assigned to the protonated structures **3a-H** and **4a-H**. All the assignments are in good agreement with the literature.[5,6,15,16] After screening experiments, we found optimal reaction conditions to be at a temperature of 80 °C and acetonitrile as solvent. We observed full conversion to the two-fold cyclized product **3a-Au** within 2 d. Lower temperatures led to a very slow conversion rate of 35% within 3 d at 50 °C, whereas higher temperatures accelerated the rearrangement (full conversion within 1 h at 150 °C). No reaction was observed within a period of 10 d when performed at room temperature.

We next sought to isolate **3a-Au** but it turned out to be sensitive towards protodeauration. For the purpose of clean analytical data, we added 1 eq. of HNTf$_2$ to **3a-Au** for complete protodeauration. Full conversion towards bench-stable **3a-H** was obtained. The crude product was purified by recrystallization in $CH_2Cl_2$/$Et_2O$ and the clean product was isolated in 83% yield. The [IPrAu][NTf$_2$] was cleanly recovered in 57% isolated yield, which might improve at large-scale reactions. $^1$H and $^{13}$C NMR spectroscopy and crystal structure analysis confirmed the anticipated connectivity and constitution (Figure 1, left). In conclusion, we were able to afford the desired structure in good yields and in a simple procedure.

With the conditions in hand, we tested the scope of the reaction. Electron-rich diynes (**1a-c**) were converted to the phosphoniumfluorenes (**3a-c**) in good to excellent yields under the standard conditions (Table 1). Electron-poor and a bulky *tert*-butyl-substituted diyne (**1d**, **1e** and **1f**) required higher temperatures or prolonged reaction times. In case of **1f**, a temperature above 100 °C was necessary and the reaction yielded a mixture of inseparable constitution isomers in a 1:2 ratio, as confirmed by X-ray single crystal structure analysis. A superimposed molecular structure of the *6-endo-dig* and the *5-exo-dig* isomers was determined (Figure 1, right, the *6-endo*-isomer was omitted for clarity). The *5-exo/6-endo* selectivity can be explained by the hyperconjugation of the alkyne π*-orbital with the vinyl gold carbenoidic carbanion in **2-Au** during the transition state. In case of terminal electron acceptors, the orbital coefficient favors the *exo*-attack, whereas with donor groups it favors the *endo*-attack.[19–21]

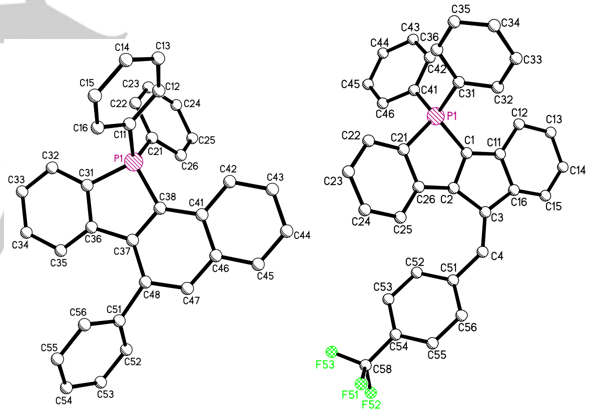

**Figure 1.** Solid state molecular structures of **3a-H** (left, twinned), **4f-H** (right, superimposed with **3f-H**).[22] Twin, superposition, counter anions, and solvent molecules are omitted for clarity.

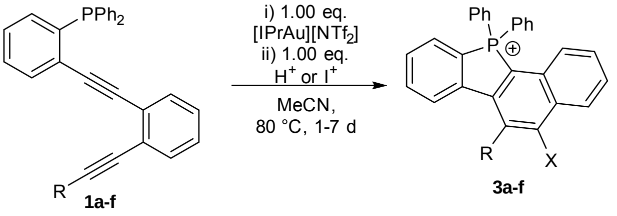

| X = H | yield | X = I | yield |
|---|---|---|---|
| **3a-H** (R = Ph) | 83%; | **3a-I** (R = Ph) | 80% |
| **3b-H** (R = *p*-Tol) | 69%; | **3b-I** (R = *p*-Tol) | 99% |
| **3c-H** (R = *p*-OMe-$C_6H_4$) | 96%; | **3c-I** (R = *p*-OMe-$C_6H_4$) | 99% |
| **3d-H** (R = *t*-Bu) | n. d.; | **3d-I** (R = *t*-Bu) | 39% |
| **3e-H** (R = *p*-F-$C_6H_4$) | 75%; | **3e-I** (R = *p*-F-$C_6H_4$) | 81% |
| **3f-Au/4f-Au** (R = *p*-$CF_3$-$C_6H_4$, X = IPrAu) ratio = 1:2, not isolated | | | |

**Table 1.** Scope. Counter anion ($NTf_2^-$) is omitted for clarity.

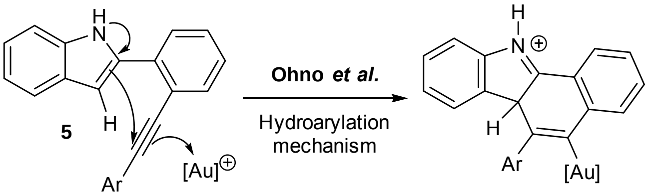

**Scheme 3.** Key elementary step for the gold(I)-catalyzed hydroarylation according to the mechanistic proposal by Ohno *et al.* Counter anions are omitted for clarity.

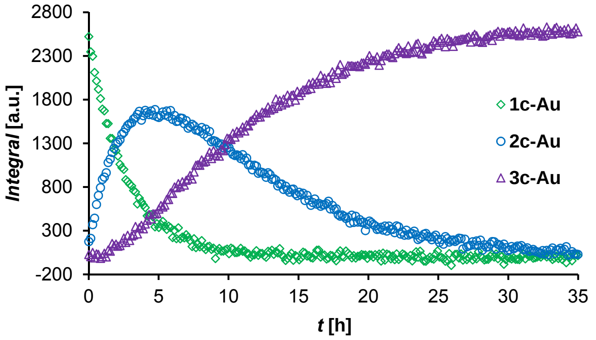

**Figure 2.** Time/conversion curve for the reaction of **1c-Au** to **3c-Au**. Conditions: **1c-Au** (20.3 µmol), [d5]-bromobenzene (0.5 mL), 80 °C.

In addition to protodeauration, $I_2$ and N-iodosuccinimide (NIS) were tested as iododeauration agents. To our delight, both reagents cleanly provided the iodinated species **3(a-e)-I** in good yields. The installation of an aryl iodine additionally allows for follow-up chemistry using simple cross-coupling methods.[23] Control experiments without gold complexes were carried out using $HNTf_2$, HCl, $B(C_6F_5)_3$,[6] Iodine[24] or NIS. All reactions were unspecific or extremely slow. With HCl, a clean reaction was observed at 80 °C, however the reaction was aborted after 19 d at 95% conversion to **3a-H**. Hence, gold(I) was found to be most efficient in this cascade.

According to mechanistic proposal for the hydroarylation of alkyne-extended indole intermediates (**5**, Scheme 3) reported by Ohno *et al*., the mechanism proceeds through electrophilic activation of the alkyne which is subsequently attacked by the indole double bond.[4] Obtaining the twofold-cyclized product **3** in the first instance was therefore surprising, as a consecutive phosphinoauration and hydroarylation would have required the protodeaurated phosphindolium intermediate. The employment of an acid, which was not added, would have been required. This prompted us to start mechanistic investigations. In order to investigate the mechanism, kinetic measurements were conducted (Figure 2 and S1). Species **2-Au** was recognized as an intermediate, which suggests that the cascade proceeds through a phosphinoauration in the initial step. The potential intermediate **2-H** was not detected by $^{31}$P NMR which can be explained by the absence of any proton source or by a fast further transformation to the aurated product in the case that traces of acid led to a protodemetallation. Based on the kinetic results, we hypothesized[25] three mechanistic pathways (1-3, Scheme 4): In each case, the reaction is induced by the thermal cleavage of the phosphane-gold bond in **1-Au** releasing the active gold complex. The gold then coordinates to either one of the alkyne bonds. In pathway 1, the rearrangement either proceeds through a phosphinoauration and protodeauration (**a**, **b**) or directly through a protophosphonylation by traces of water (**c**), yielding **2-H** as intermediate. This is followed by a gold-catalyzed hydroarylation (**d**), which is consistent with the mechanistic proposal of Ohno *et al.* made during their investigation on polyyne cascades.[4] In order to check pathway 1, **2a-H** was synthesized by the *protophosphonylation* of **1a** with 1 eq. of $HNTf_2$. The consecutive transformation to **3a-H** was attempted, however neither the addition of catalytic nor stoichiometric amounts of [IPrAu][$NTf_2$] gave a further conversion at temperatures between 80 °C and 150 °C within 5 d (even under basic conditions using DBU, Scheme 5a). These results account for an irreversible formation of **2-H** which was again confirmed by another control experiment: In the presence of the phosphindolium complex **2e-H**, the complex **1c-Au** was transformed into **3c-Au**. While **1c** was fully converted to **3c**, **2e-H** remained completely unaffected demonstrating that **2-H** is not involved in the reaction (Scheme 5b). In conclusion, Ohno's mechanism seems not to be operative. Please note that the phospholium double bond in **2-H** is less nucleophilic than in indoles and therefore its attack might be unfavored. In pathway 2, the mechanism proceeds through a concerted diyne cyclization[26,27] generating a phenyl cation (**e**), which represents the zwitterionic version of the Bergmann cyclization[20,21]. For the diyne mechanism we anticipated a dramatic increase of the reaction velocity in the presence of the free gold(I). However, the velocity did not substantially increase when 2 eq. of [Au]$^+$ were used.

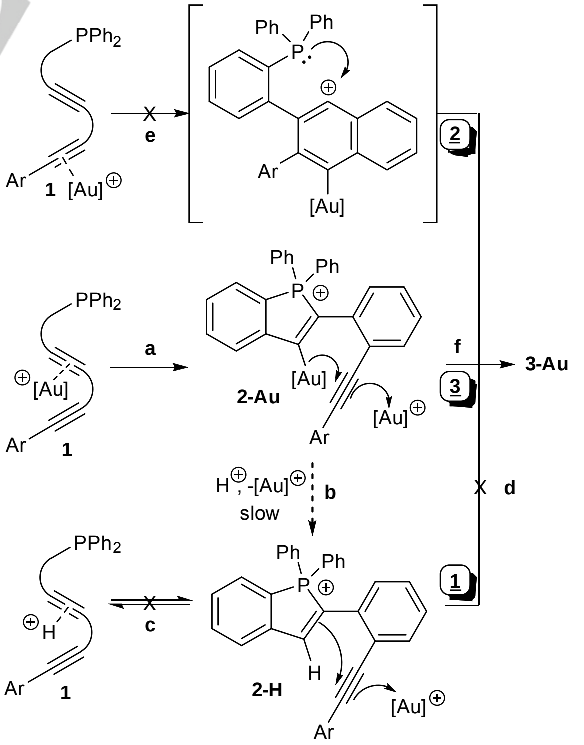

**Scheme 4.** Overview of stoichiometric reaction pathways under standard conditions. Counter anions are omitted for clarity.

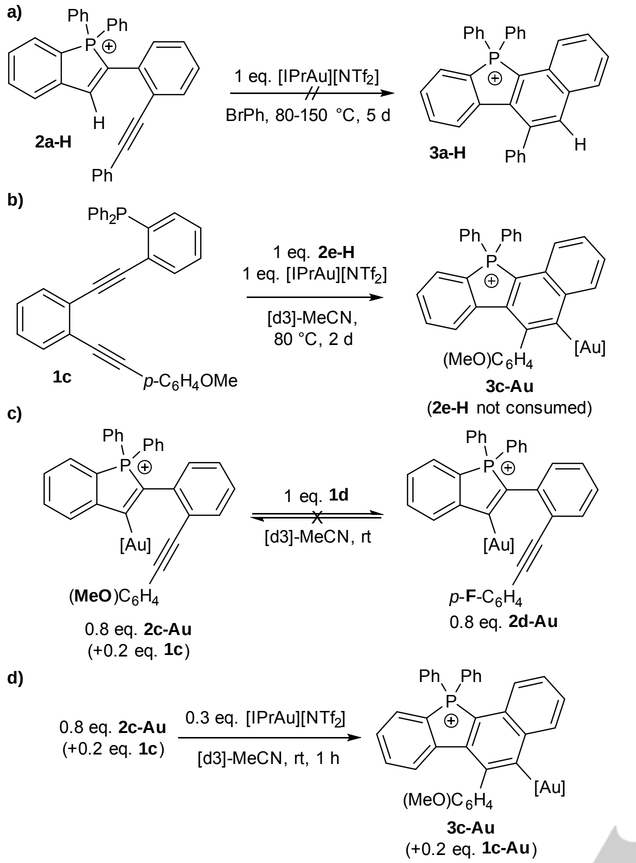

**Scheme 5. a)** Gold-mediated conversion of **2a-H** in **3a-H** (pathway 1). **b)** Conversion of **1c** in presence of **2e-H** (pathway 1). **c)** Equilibration experiment (pathway 2) **d)** Gold-catalyzed conversion of **2c-Au** in **3c-Au** (pathway 3).

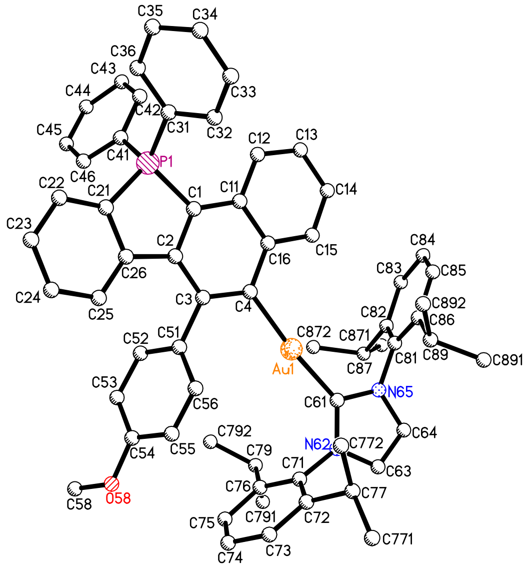

**Figure 3.** Solid state molecular structure of **3c-Au**.[22] Selected bond lengths [Å] and angles [°]:Au1-C61 2.029(3), Au1-C4 2.050(3), P1-C1 1.781(3), P1-C21 1.780(3), C21-C26 1.407(4), C2-C26 1.497(4), C1-C2 1.393(4), C2-C3 1.420(4), C3-C4 1.398(4); C61-Au1-C4 174.37(11), C21-P1-C1 94.01(13), C2-C1-P1 109.48(19), C26-C21-P1 109.3(2), C2-C3-C51 119.7(2), C31-P1-C41 110.11(14). Counter anions, and solvent molecules are omitted for clarity.

Furthermore, a reversible reaction from the phosphindolium species **2-Au** to **1-Au** would be necessary for pathway 2 in order to match the kinetic results. However, the reversibility of the formation of **2-Au** was disproven in a stepwise experiment using the phosphindolium gold complex as starting material (Scheme 5c). First, **2c-Au** was generated reacting 0.8 eq. of [IPrAu][[NTf$_2$] with 1 eq. of **1c** at 80 °C. Subsequently, 1 eq. of **1e** was added and the sample was further heated at 80 °C. The formation of **2e-Au** that would have been expected in case of a reverse reaction was not observed. This result indicates that **1-Au** and **2-Au** are not in equilibrium and hence that the diyne mechanism does not apply. These results can be rationalized by the strong coordination of the gold center to the phosphane moiety restricting the full spectrum of the gold's reactivity. Over the diyne mechanism, the phosphinoauration presumably is preferred due to the proximity of the corresponding alkyne bond. In case of the reaction with 2 eq. of [IPrAu][NTf$_2$], the phosphane is occupied as a nucleophile which prevents a successful Bergmann cyclization. Interestingly, when using 2 eq. of [IPrAu][NTf$_2$], the germinal diaurated species was not observed. Presumably, its formation is unfavored due to the electron-deficiency of the phosphoniumfluorene.[27]
In pathway 3, a phosphinoauration leads to **2-Au** (**a**) first, but instead of protodeauration, the alkyne-activation by a second [Au]-center triggers the nucleophilic attack in a direct fashion (**f**). Please note that a concerted *trans*-addition with a single [Au]-center in **2-Au** would be geometrically impossible. The phosphindolium-gold complex **2c-Au** was synthesized from **1c** using 0.8 eq. of [IPrAu][NTf$_2$] at 80 °C. After the full conversion of the [IPrAu][NTf$_2$], an excess of 10 mol% [IPrAu][NTf$_2$] was generated by the addition of further 0.3 eq. (the remaining 0.2 eq. were consumed by the complexation with the residual **1c**). Herein, a complete conversion of **2c-Au** to **3c-Au** was observed after 1 h at room temperature (Scheme 5d). The corresponding molecular structure of **3c-Au** in the solid state was confirmed by single crystal X-ray structure analysis (Figure 3). Similar results were obtained by adding 0.5 or 1 eq. of HNTf$_2$ to **2c-Au**. The addition led to full conversion to **3c** in less than 1 h at room temperature. On basis of these results, we propose a mechanism proceeding through gold exchange. We conclude that in our experiments **2c-Au** underwent protodeauration in catalytic quantities. The released [Au] then activated the remaining alkyne bond and the vinyl-gold electron pair attacked the activated carbon atom under exchange of the [Au]-center. Thus, the second step of the sequence is gold-catalyzed. In context of the work by Ohno *et al.*, the experiments clearly demonstrate a higher nucleophilicity of the vinyl-gold versus the vinyl-H electron pair which to the best of our knowledge was not investigated before. This changes the mechanistic view of gold-catalyzed hydroarylations: Beside the mechanistic proposal by Ohno *et al.*, the contribution of the gold-exchange mechanism has to be considered for electron-poor aromatics.

Next, the material properties were investigated and CV measurements were conducted. A representative cyclic voltammogram of **3a-H** is depicted in Figure 4. For the protonated fluorenes **3a-H**, **3b-H**, and **3e-H**, potentials of $E_p$ = -1.7 V were recorded which are about 0.2 V lower than the literature values for the methyl phenyl phosphoniumfluorene.[28] For the iodinated fluorenes **3b-I** and **3e-I**, a two-electron acceptance was observed at potentials of $E_{p1}$ = -1.5 V and $E_{p2}$ = -1.7 V. A representative cyclic voltammogram of **3b-I** is depicted in Figure 5. All compounds were found to be irreversibly reduced as indicated by the $\Delta E_p$ values and the $I_{p,Ox}/I_{p,Red}$-ratios (see SI).

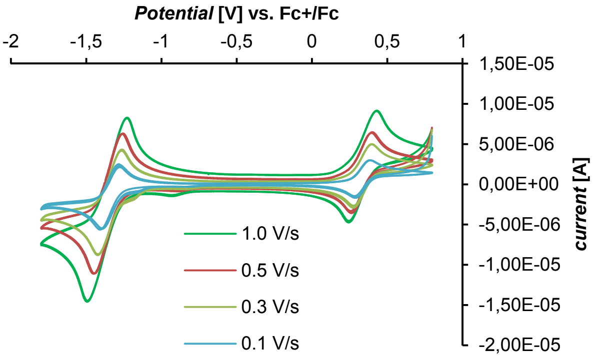

**Figure 4.** Cyclic voltammogram of **3a-H** at different scan rates.

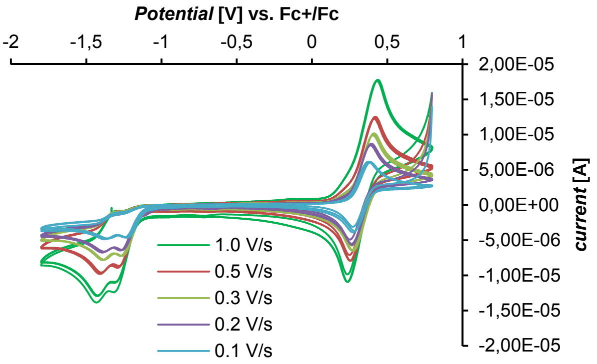

**Figure 5.** Cyclic voltammogram of **3b-I** at different scan rates.

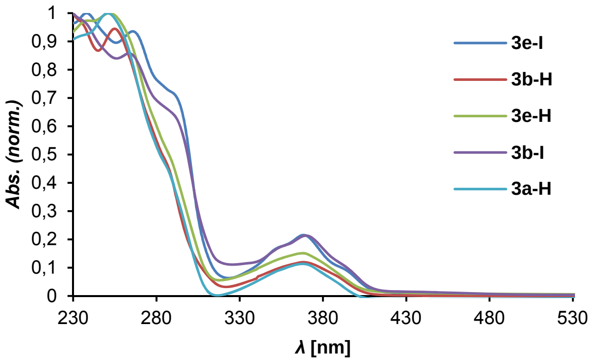

**Figure 6.** UV-Vis spectra of compounds **3a-H**, **3b-H**, **3b-I**, **3e-H**, and **3e-I**.

By UV-Vis spectroscopy a strong absorbance was observed in the UV region with absorption maxima at 251 nm, 254 nm, and 252 nm for **3a-H**, **3b-H**, and **3e-H** (Figure 6). For these structures, a small shoulder was noticed at around 289 nm. **3b-I** and **3e-I** showed maxima at 264 nm and 265 nm with a larger shoulder at 287 nm. For all compounds, a second absorption band is observed in the visible region with maxima between 367 nm and 370 nm. The iodinated structures additionally show two distinct shoulders at 353 nm and 390 nm. The LUMO levels and HOMO levels for **3** were estimated based on the CV and UV-Vis measurements. The LUMO and HOMO levels for the protonated compounds **3a-H**, **3b-H**, and **3e-H** were approximated to $E_{LUMO}$ = -3.11 eV and $E_{HOMO}$ = -6.49 eV. For **3b-I** and **3e-I**, they were approximated to $E_{LUMO}$ = -3.3 eV and $E_{HOMO}$ = -6.7 eV. All compounds showed a similar HOMO-LUMO gap of $E_{gap}$ = 3.4 eV. TDDFT calculations showed good agreement with the measured values ($E_{gap}$ = 3.7 eV for **3a-H**, CAM-B3LYP/Def2TZVPP, see SI). The values for the HOMO-LUMO gaps suggest a potential application for these materials as a hole-blocking layer (HBL) in solar cells.

The phosphoniumfluorene structure **3c-H** was tested as a HBL in inverted architecture perovskite solar cells (Figure 7a). As perovskite material, $CH_3NH_3PbI_3$ ($MAPbI_3$) was used, while [6,6]-phenyl-C61-butyric acid methyl ester (PCBM) was used as electron transport layer. Inverted architecture perovskite solar cell means that in this architecture the indium tin oxide (ITO) is the anode, whereas the metal contact constitutes the cathode. **3c-H** devices were compared to devices without a HBL and with the commonly used bathocuproine (BCP).[29,30] Summarizing the results of the CV, UV-Vis, and the ultraviolet photoemission spectroscopy (UPS) measurements, the corresponding energy diagram of the solar cell is shown in Figure 7b. Compared to the PCBM HOMO level, the low-lying HOMO level of **3-H** can effectively block the holes from the PCBM to the metal contacts. Figure 7c shows the J-V curves obtained from the three types of devices. Devices without HBL show a reduced performance with a characteristic S-shape of the J-V curve that originates from the increased series resistance of the device.[31] Additionally, devices without a HBL show a minor hysteresis. In comparison, devices with **3c-H** as a HBL show a significantly improved photovoltaic performance, reaching a power conversion efficiency (PCE) of 14.17%. The devices exhibit a higher fill factor (FF), a much lower series resistance (Rs), and show nearly no hysteresis. Reference devices with BCP as HBL show a very similar performance to those with **3c-H**, demonstrating that the phosphoniumfluorene structure can be effectively applied as hole blocking layer in perovskite solar cells. The photovoltaic parameters and the extracted series resistances are summarized in Table 2.

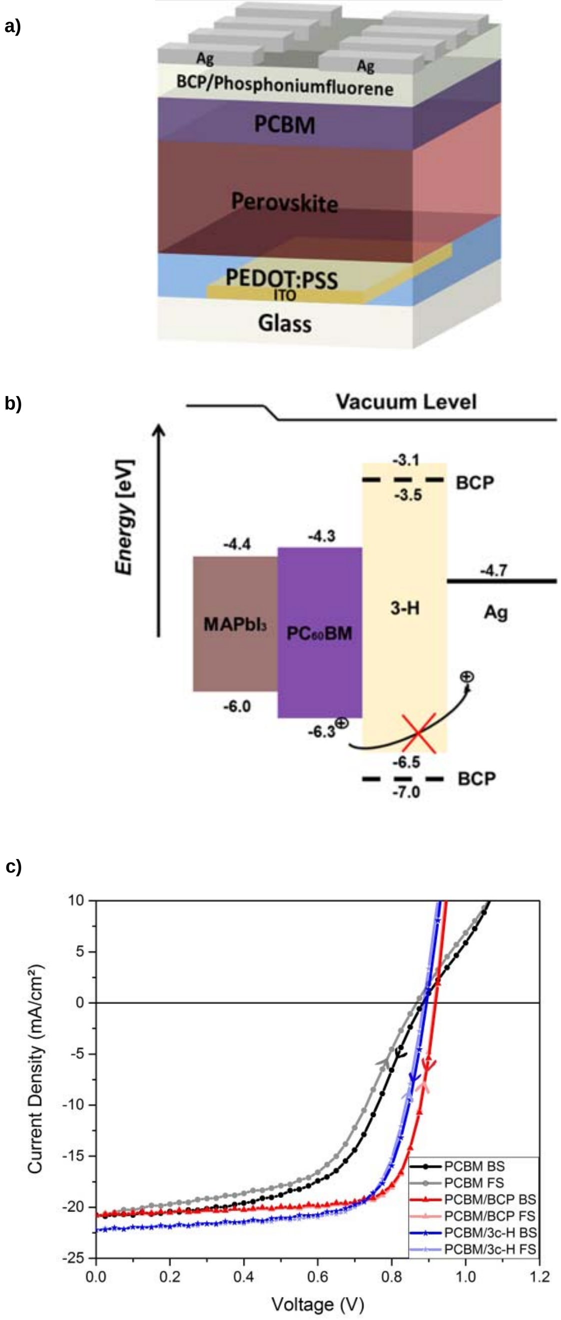

**Figure 7.** (a) Perovskite solar cell device structure. (b) Energy diagram of Perovskite/PCBM/hole blocking layer/Ag. UPS was used to determine the HOMO and LUMO levels of $MAPbI_3$ and PCBM in a thin film. (c) J-V curves of devices with and without different hole blocking materials. Both reverse and forward scan directions are shown.

**Table 2.** Photovoltaic performance parameters with and without BCP or **3c-H** as HBL for both reverse and forward scan directions. Rs was extracted from the J-V curve at V = $V_{oc}$.

| | scan direction | $V_{oc}$ (V) | $J_{sc}$ (mA/cm$^3$) | FF (%) | PCE (%) | Rs (Ωcm$^2$) |
|---|---|---|---|---|---|---|
| **PCBM** | Backward | 0.88 | -20.74 | 58.23 | 10.68 | 17.25 |
| | Forward | 0.87 | -20.74 | 55.3 | 9.95 | |
| **PCBM/BCP** | Backward | 0.92 | -20.81 | 76.64 | 14.60 | 3.99 |
| | Forward | 0.92 | -20.81 | 75.27 | 14.39 | |
| **PCBM/3c-H** | Backward | 0.89 | -22.22 | 71.93 | 14.17 | 3.98 |
| | Forward | 0.89 | -22.22 | 70.89 | 14.09 | |

## Conclusions

In summary, we developed the domino synthesis of $\pi$-extended phosphoniumfluorenes in a simple procedure and with up to quantitative yields. The gold-complex could be recovered which increases the efficiency. Furthermore, the electron-deficient nature of the phosphoniumfluorene allowed the trapping of the key-intermediates in the mechanism, which resulted in the determination of the "gold-exchange mechanism". The reaction accordingly follows a phosphinoauration in the first step leading to the phosphindolium-gold complex. The remaining triple bond is then activated by a second gold-center which triggers the *6-endo-dig* cyclization to the phosphoniumfluorene under exchange of the gold centers. Hence, the *6-endo-dig* cyclization in the second step is gold-catalyzed, whereas the phosphinoauration requires stoichiometric amounts of gold. Our finding regarding the gold-exchange mechanism provides a new perspective by means of gold-catalyzed hydroarylation reactions and thus is significant for future developments in this field. TDDFT calculations, CV, UV-Vis measurements, and the application in solar cell devices show that phosphoniumfluorenes are promising candidates to be applied as efficient hole blocking layer materials in perovskite photovoltaics. As part of our interest in gold-catalysis, the development of a catalyzed phosphinoauration is under investigation. This requires an efficient deauration mechanism which neither interferes with the gold-catalytic cycle nor leaves a strongly coordinating anion that effectively inhibits the gold-catalyst.

## Experimental Section

**General Procedure for the Cyclization Cascade:** Under argon atmosphere, the phosphane-substituted enediyne and the given amount of [IPrAu][$NTf_2$] were dissolved in 0.5 mL solvent. The mixture was transferred to a Young-NMR tube and heated at the described temperature. The reactions were monitored using $^{31}$P NMR spectroscopy and upon complete conversion, the reaction mixture was treated with a deauration agent (i. e. $HNTf_2$ or NIS). The solvent was removed under reduced pressure and the crude product was recrystallized in a mixture of $CH_2Cl_2$/$Et_2O$/n-pentane (1:5:5 v/v/v, 15 mL, -20 °C). For large-scale reactions, precipitation in $CH_2Cl_2$/$Et_2O$ is sufficient. The crystals were filtered off and washed with pentane to obtain the pure product. Alternatively, the crude product can be purified by flash column chromatography on silica gel (pure PE to pure $Et_2O$) and by subsequent extraction with $CH_2Cl_2$/$H_2O$ and with MeCN/pentane.

**General Procedure for the Fabrication and Characterization Perovskite Solar Cell:** ITO coated glass substrates were ultrasonic cleaned by acetone and isopropanol for 10 min, followed by 10 min plasma treatment. PEDOT:PSS was spin coated on cleaned ITO substrate with 150 °C 15 min annealing. Lead acetated trihydrate perovskite solution was spin coated onto PEDOT:PSS in a drybox (RH < 5%) with drying 5 min and 100 °C 5 min annealing.[29] The prepared samples were transferred into a $N_2$ filled glovebox. Subsequently, PCBM in chlorobenzene (20 mg/ml) and BCP(0.5 mg/ml)/**3c-H**(1 mg/ml) in isopropanol was dynamically spin-coated on the samples at 2000 rpm and 4000 rpm, respectively. To complete the device, 80 nm silver electrode was deposited via thermal evaporation under high-vacuum. The J–V measurements were performed under simulated AM 1.5 sunlight at 100 mW cm$^{-2}$ irradiance (Abet Sun 3000 Class AAA solar simulator) with a Keithley 2450 Source Measure Unit. The light intensity was calibrated with a Si reference cell (NIST traceable, VLSI).

## Acknowledgements

SA and PWA thank Florian F. Mulks for computational advices. QA and YV thank the DFG for financial support (SFB 1249, Project C04).

**Keywords:** Protophosphonylation • Phosphinoauration • enediyne cyclization • domino reaction • cascade • hole blocking layer • perovskite solar cells

[1] D. E. Fogg, E. N. dos Santos, *Coord. Chem. Rev.* **2004**, *248*, 2365–2379.

[2] a) L. F. Tietze, U. Beifuss, *Angew. Chem. Int. Ed.* **1993**, *32*, 131–163; b) L. F. Tietze, U. Beifuss, *Angew. Chem.* **1993**, *105*, 137–170.

[3] a) P. M. Byers, J. I. Rashid, R. K. Mohamed, I. V. Alabugin, *Org. Lett.* **2012**, *14*, 6032–6035; b) A. S. K. Hashmi, I. Braun, M. Rudolph, F. Rominger, *Organometallics* **2012**, *31*, 644–661; for reviews, see: c) G. Dyker, *Angew. Chem. Int. Ed.* **2000**, *39*, 4237–4239; d) G. Dyker, *Angew. Chem.* **2000**, *112*, 4407–4409; e) A. S. K. Hashmi, *Chem. Rev.* **2007**, *107*, 3180–3211; f) A. M. Asiri, A. S. K. Hashmi, *Chem. Soc. Rev.* **2016**, *45*, 4471–4503; g) D. Pflästerer, A. S. K. Hashmi, *Chem. Soc. Rev.* **2016**, *45*, 1331–1367.

[4] K. Hirano, Y. Inaba, N. Takahashi, M. Shimano, S. Oishi, N. Fujii, H. Ohno, *J. Org. Chem.* **2011**, *76*, 1212–1227.

[5] S. Arndt, M. M. Hansmann, P. Motloch, M. Rudolph, F. Rominger, A. S. K. Hashmi, *Chem. Eur. J.* **2017**, *23*, 2542–2547.

[6] S. Arndt, M. M. Hansmann, F. Rominger, M. Rudolph, A. S. K. Hashmi, *Chem. Eur. J.* **2017**, *23*, 5429–5433.

[7] a) F. Riobé, R. Szücs, C. Lescop, R. Réau, L. Nyulászi, P.-A. Bouit, M. Hissler, *Organometallics* **2017**, *36*, 2502–2511; b) T. Baumgartner, *Acc. Chem. Res.* **2014**, *47*, 1613–1622; c) J. Yin, R.-F. Chen, S.-L. Zhang, Q.-D. Ling, W. Huang, *J. Phys. Chem. A* **2010**, *114*, 3655–3667.

[8] Y. Matano, H. Imahori, *Org. Biomol. Chem.* **2009**, *7*, 1258–1271.

[9] a) G. Wittig, A. Maercker, *Chem. Ber.* **1964**, *97*, 747–768; b) I. G. M. Campbell, R. C. Cookson, M. B. Hocking, A. N. Hughes, *J. Chem. Soc.* **1965**, 2184.

[10] R. Rothuis, J. J. H. M. F. Freide, J. M. F. van Dijk, H. M. Buck, *Recl. Trav. Chim. Pays-Bas* **1974**, *93*, 128–129.

[11] D. Marcoux, A. B. Charette, *J. Org. Chem.* **2008**, *73*, 590–593.

[12] a) D. Marcoux, A. B. Charette, *Adv. Synth. Catal.* **2008**, *350*, 2967–2974; b) L. Horner, G. Mummenthey, H. Moser, P. Beck, *Chem. Ber.* **1966**, *99*, 2782–2788.

[13] E. Rémond, A. Tessier, F. R. Leroux, J. Bayardon, S. Jugé, *Org. Lett.* **2010**, *12*, 1568–1571.

[14] A. F. Fearnley, J. An, M. Jackson, P. Lindovska, R. M. Denton, *Chem. Commun.* **2016**, *52*, 4987–4990.

[15] K. Baba, M. Tobisu, N. Chatani, *Angew. Chem. Int. Ed.* **2013**, *52*, 11892–11895.

[16] K. Baba, M. Tobisu, N. Chatani, *Angew. Chem.* **2013**, *125*, 12108–12111.

[17] M. Widhalm, C. Aichinger, K. Mereiter, *Tetrahedron Lett.* **2009**, *50*, 2425–2429.

[18] Q. Ge, J. Zong, B. Li, B. Wang, *Org. Lett.* **2017**, *19*, 6670–6673.

[19] K. Gilmore, R. K. Mohamed, I. V. Alabugin, *WIREs Comput Mol Sci* **2016**, *6*, 487–514.

[20] G. Dos Passos Gomes, I. V. Alabugin, *Journal of the American Chemical Society* **2017**, *139*, 3406–3416.

[21] P. W. Peterson, R. K. Mohamed, I. V. Alabugin, *Eur. J. Org. Chem.* **2013**, *2013*, 2505–2527.

[22] CCDC-1587137 (**3a-H**), CCDC-1587190 (**4f-H**), CCDC-1587135 (**3c-Au**) contain the supplementary crystallographic data for this paper. These data can be obtained free of charge from The Cambridge Crystallographic Data Centre via www.ccdc.cam.ac.uk/data_request/cif.

[23] a) M. T. Reetz, G. Lohmer, R. Schwickardi, *Angew. Chem. Int. Ed.* **1998**, *37*, 481–483; b) M. T. Reetz, G. Lohmer, R. Schwickardi, *Angew. Chem.* **1998**, *110*, 492–495; c) X. Zhao, Z. Gan, C. Hu, Z. Duan, F. Mathey, *Org. Lett.* **2017**, *19*, 5814–5817.

[24] C.-C. Chen, S.-C. Yang, M.-J. Wu, *J. Org. Chem.* **2011**, *76*, 10269–10274.

[25] a) A. S. K. Hashmi, *Angew. Chem. Int. Ed.* **2010**, *49*, 5232–5241; b) A. S. K. Hashmi, *Angew. Chem.* **2010**, *122*, 5360–5369.

[26] a) N. Villegas-Escobar, M. H. Larsen Née Vilhelmsen, S. Gutiérrez-Oliva, A. S. K. Hashmi, A. Toro-Labbé, *Chem. Eur. J.* **2017**, *23*, 13360–13368; b) M. Wieteck, M. H. Larsen Née Vilhelmsen, P. Nösel, J. Schulmeister, F. Rominger, M. Rudolph, M. Pernpointner, A. S. K. Hashmi, *Adv. Synth. Catal.* **2016**, *358*, 1449–1462; c) M. H. Larsen, K. N. Houk, A. S. K. Hashmi, *J. Am. Chem. Soc.* **2015**, *137*, 10668–10676; d) M. H. Vilhelmsen, A. S. K. Hashmi, *Chem. Eur. J.* **2014**, *20*, 1901–1908; e) M. M. Hansmann, S. Tšupova, M. Rudolph, F. Rominger, A. S. K. Hashmi, *Chem. Eur. J.* **2014**, *20*, 2215–2223.

[27] for a review, see: Braun, Ingo, A. M. Asiri, A. S. K. Hashmi, *ACS Catal.* **2013**, *3*, 1902–1907.

[28] P. Adkine, T. Cantat, E. Deschamps, L. Ricard, N. Mézailles, P. Le Floch, M. Geoffroy, *Phys. Chem. Chem. Phys.* **2006**, *8*, 862–868.

[29] Q. Sun, P. Fassl, D. Becker-Koch, A. Bausch, B. Rivkin, S. Bai, P. E. Hopkinson, H. J. Snaith, Y. Vaynzof, *Adv. Energy Mater.* **2017**, *7*, 1700977.

[30] C. Chen, S. Zhang, S. Wu, W. Zhang, H. Zhu, Z. Xiong, Y. Zhang, W. Chen, *RSC Adv.* **2017**, *7*, 35819–35826.

[31] Z. Lin, J. Chang, J. Xiao, H. Zhu, Q.-H. Xu, C. Zhang, J. Ouyang, Y. Hao, *Sol. Energ. Mat. Sol. Cells.* **2016**, *157*, 783–790.

# FULL PAPER

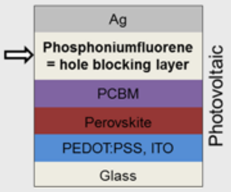

A domino reaction to phosphoniumfluorenes with up to quantitative yields was developed. Mechanistic studies support the proposal of a gold-exchange mechanism. The properties were investigated by CV, UV-Vis, and TDDFT studies. The material was tested as a hole blocking layer in perovskite solar cells.

*Sebastian Arndt,[a] Jan Borstelmann,[a] Rebeka Eshagh Saatlo,[a] Patrick W. Antoni,[a] Frank Rominger,[a] Matthias Rudolph,[a] Qingzhi An,[b,c] Yana Vaynzof,*[b,c] and A. Stephen K. Hashmi*[a,d]*

***Page No. – Page No.***

**The Gold(I)-Mediated Domino Reaction to Fused Diphenyl Phosphoniumfluorenes: Mechanistic Consequences for Gold-Catalyzed Hydroarylations and the Application in Solar Cells**